Volume 3
Number 8
August 2023
Pages 1127–1244

Environmental Science Atmospheres

rsc.li/esatmospheres

ISSN 2634-3606

ROYAL SOCIETY OF CHEMISTRY

PAPER

Johannes Passig *et al.*

Detection of ship emissions from distillate fuel operation *via* single-particle profiling of polycyclic aromatic hydrocarbons

Environmental Science: Atmospheres

ROYAL SOCIETY OF CHEMISTRY

PAPER

View Article Online
View Journal | View Issue

Open Access Article. Published on 12 July 2023. Downloaded on 11/22/2025 9:57:57 PM.
This article is licensed under a Creative Commons Attribution-NonCommercial 3.0 Unported Licence.

Check for updates

Cite this: *Environ. Sci.: Atmos.*, 2023, **3**, 1134

Detection of ship emissions from distillate fuel operation *via* single-particle profiling of polycyclic aromatic hydrocarbons†

Lukas Anders,[abc] Julian Schade,[abce] Ellen Iva Rosewig,[abc] Thomas Kröger-Badge,[ab] Robert Irsig,[cd] Seongho Jeong,[abc] Jan Bendl,[e] Mohammad Reza Saraji-Bozorgzad,[abde] Jhih-Hong Huang,[f] Fu-Yi Zhang,[f] Chia C. Wang,[f] Thomas Adam,[abe] Martin Sklorz,[ab] Uwe Etzien,[g] Bert Buchholz,[g] Hendryk Czech,[ab] Thorsten Streibel,[abc] Johannes Passig *[abc] and Ralf Zimmermann[abc]

Received 17th April 2023
Accepted 12th July 2023

DOI: 10.1039/d3ea00056g

rsc.li/esatmospheres

Using novel ionization technologies in single-particle mass spectrometry (SPMS), we analyzed the polycyclic aromatic hydrocarbons (PAHs) on individual particles from a research ship engine running on marine gasoil (MGO). We found a rather uniform PAH signature on the majority of particles. The PAH pattern is stable for all engine loads and particle sizes and differs from typical signatures of other pyrogenic and petrogenic PAH sources. Based on this observation, we conducted a field experiment and observed that the appearance of this PAH signature is associated with marine air masses. Moreover, we could detect the plume of a single ship passage at 15–20 km distance by the transient appearance of particles with the same distinct PAH profile. Consequently, we suggest the use of the specific PAH pattern as a new marker to detect and monitor ship emissions, independent of the conventional metal signatures that are not applicable for compliant fuels in emission control areas and coastal waters.

Environmental significance

Air pollution from ships affects the atmospheric environment, with substantial impact on public health and climate. Emission control areas (ECAs) were installed worldwide to protect coastal regions against ship emissions by limiting the fuel's sulfur content. In ECAs, the traditional bunker fuels are replaced by *e.g.* marine gasoil, which also produces aerosols with severe health effects. Such distillate fuels do not contain metals from the refinery process. Thus, the traditional marker concept for ship emissions becomes obsolete because it is based on these metals. Ship emission detection, source apportionment and risk assessment therefore require novel marker concepts. Here we target this gap by introducing a new method to detect ship emission particles by using their content of polycyclic aromatic hydrocarbons.

Introduction

The marine transport sector is a major contributor to the global burden of air pollution. While nearly all air pollutants in Europe and the U.S. have decreased within the last few decades, ship emissions have changed less and currently contribute substantially to the total emissions of PM 2.5.[1–7] Regulations target the fuel sulfur content by a global 0.5% sulfur cap since 2020 and a maximum of 0.1% S in sulfur emission control areas (SECAs), *e.g.* along the U.S. coast, the entire North Sea and Baltic Sea as well as in many harbors and coastal regions worldwide.[8] Shipowners can either switch to compliant low-sulfur fuels (*e.g.* marine gasoil and MGO) or install an exhaust cleaning device ('scrubber'), allowing them to use the cheaper high-sulfur heavy fuel oils also in SECAs.[9,10] While the sulfur regulations and the resulting changes to cleaner fuels reduced total particulate matter emissions with benefits for ecosystems and human health,[11–13] the use of scrubbers can have collateral effects on the environment.[10,14–16] Beyond the sulfur aspect, the fuel type strongly affects the physical and chemical properties of the emissions[17–19] and their health effects.[20,21] Most ships in SECAs currently operate with MGO;[9]

[a]Joint Mass Spectrometry Centre, Department of Analytical and Technical Chemistry, University of Rostock, 18051 Rostock, Germany. E-mail: johannes.passig@uni-rostock.de

[b]Comprehensive Molecular Analytics, Helmholtz Centre Munich, 85764 Neuherberg, Germany

[c]Department Life, Light & Matter, University of Rostock, 18051 Rostock, Germany

[d]Photonion GmbH, 19061 Schwerin, Germany

[e]Faculty for Mechanical Engineering, Institute of Chemistry and Environmental Engineering, University of the Bundeswehr Munich, 85577 Neubiberg, Germany

[f]Department of Chemistry and Aerosol Science Research Center, National Sun Yat-sen University, Kaohsiung, Taiwan 804, Republic of China

[g]Chair of Piston Machines and Internal Combustion Engines, University of Rostock, Germany

† Electronic supplementary information (ESI) available. See DOI: https://doi.org/10.1039/d3ea00056g

© 2023 The Author(s). Published by the Royal Society of Chemistry

Open Access Article. Published on 12 July 2023. Downloaded on 11/22/2025 9:57:57 PM. This article is licensed under a Creative Commons Attribution-NonCommercial 3.0 Unported Licence.

however, the use of these cleaner fuels without filter technologies also produces severe health effects.[21]

Estimates of the burden of air pollution from ships are mainly based on laboratory/on-ship studies[18,22,23] and transport modelling.[24] Monitoring of ship plumes under clean air conditions is possible through gas phase measurements[25–27] and transient increases in particle number concentrations, black carbon or SO_x.[28,29] However, in populated coastal regions with complex aerosols, source apportionment relies on chemical markers for shipping, usually combinations of the transition metals vanadium(V), nickel (Ni) and iron (Fe).[30–32]

Single-particle mass spectrometry (SPMS) detects these particle-bound metals in real time,[33–36] and hence, it is applicable for monitoring ship emissions and source apportionment in complex environments.[37–40] Recently, the sensitivity of SPMS to metals has been increased by exploiting laser-atom resonances.[41] With this approach, individual ship plumes have been detected in an urban background from >10 km distance, and also from ships with scrubbers installed.[42]

Of note, source apportionment based on transition metals is only applicable if the ships run on residual fuels or on partly residual fuels such as marine diesel oil. For the distillate fuels that dominate in SECAs and gain importance in the course of the new global regulations, novel marker approaches based on polycyclic aromatic hydrocarbons (PAHs) have been suggested.[43,44] In parallel, new ionization methods for SPMS were introduced, yielding detailed mass spectra of PAHs in addition to the particle's inorganic composition.[45,46] Consequently, the combination of the novel single-particle PAH analyses with PAH marker concepts opens new avenues for source apportionment.

Here we present the first study applying single-particle mass spectrometry to investigate the fresh emissions of a ship engine. We used the recently developed SPMS techniques that reveal signatures of PAHs on a single-particle basis.[46] Thus, we were able to evaluate and establish the predicted PAH markers for MGO combustion on ships. To prove this new concept for source apportionment of ship emissions under real-world conditions, we present the first detection of a ship plume by using PAH emissions.

Methods

Ship engine and sampling

The laboratory experiments were conducted using a one-cylinder four-stroke 80 kW research ship engine with common rail injection. The engine is a well-documented model for ship propulsion systems,[47] capable of operating with all common ship fuels; for details see Streibel *et al.*[18] Four different operating points were investigated: 100, 75, 50 and 25% load, each for one hour and with a run-in time of 25 min for stabilization. The aerosol was sampled, and transported through a cyclone separator (cutoff diameter 10 μm) at a temperature of 200 °C. Using a two-stage ejector dilution system (eDiluter, Dekati Ltd., Finland), the aerosol was cooled to room temperature and diluted by a factor of 1 : 25 with clean, dried and particle-free air. From 1 L min^{-1} aerosol transported to the SPMS system, 0.1 L min^{-1} was guided into the instrument. Further details of the sampling setup were given by Jeong *et al.*[7]

SPMS instrumentation

The new laser ionization scheme for combined measurements of inorganic composition and PAHs has been described in detail in another publication.[46] The instrument and parameters were not changed. In brief, the particles are accelerated and focused by an aerodynamic lens system before optical detection and sizing. When entering the ion source of the mass spectrometer, each detected particle is exposed to an IR pulse for laser desorption (LD) of the organic material. An unfocused UV beam (λ = 248 nm) from a KrF excimer laser intersects the expanding gaseous plume, inducing resonance-enhanced multiphoton ionization (REMPI) of PAHs in the plume. The laser beam is back-reflected and focused into the center of the plume, where it hits the particle residue for laser desorption/ionization (LDI) of inorganic and refractory particle compounds at high laser intensities (~2 GW cm^{-2}). The positive flight tube of the mass analyzer detects the PAHs together with cations from LDI, while the opposite negative flight tube measures anions from LDI. Ion signals were recorded with a 14-bit digitizer (ADQ14, Teledyne SP Devices AB, Sweden) and custom LabView software. Note that in SPMS, the peak height is not directly convertible to the mass concentration of a specific substance. The new method applied here yields PAH mass spectra from individual particles; however, it cannot distinguish between isobar substances, *e.g.* phenanthrene *vs.* anthracene or benzo[*a*]pyrene *vs.* perylene.

Analysis of single-particle mass spectra

For the clustering of mass spectral signatures, we used the adaptive resonance theory neural network algorithm, ART-2a.[48] The program code was taken from the open-source toolkit FATES[49] and embedded in custom Matlab software (MathWorks Inc.). With regard to the different ionization processes, LDI and REMPI mass spectra were separately normalized and independently clustered using a vigilance factor of 0.8, a learning rate of 0.05, and 20 iterations.[50] In order to identify the main particle classes, we applied a regrouping algorithm, where clusters from the initial clustering are merged in a second ART-2a run.[51] The results were regularly cross-checked against those of manual merging.

Ambient air sampling

The field experiments shown here were part of a measurement campaign at the Swedish West coast.[50] The clean air conditions there required aerosol preconcentration (Model 4240, MSP corp., USA)[52] and drying (Model MD-700-12S-1, Perma Pure LLC, U.S.). Wind data were acquired from the local station Nidingen, 8 km south of the sampling site.[53]

Results and discussion

Particle types emitted by the laboratory ship engine

First, we investigated the ship engine's exhaust aerosol with respect to the single-particle chemical composition of inorganic

Open Access Article. Published on 12 July 2023. Downloaded on 11/22/2025 9:57:57 PM.
This article is licensed under a Creative Commons Attribution-NonCommercial 3.0 Unported Licence.

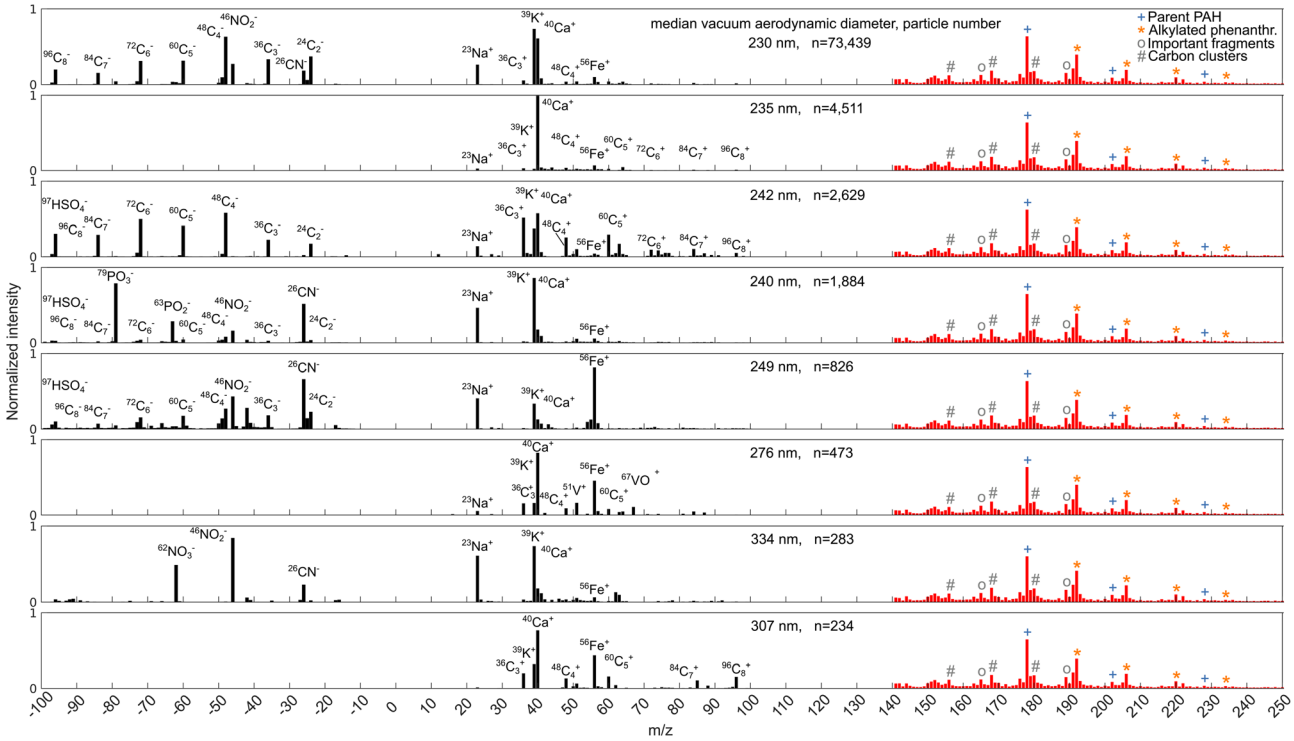

Fig. 1 Mass spectra of the eight main particle classes from ART2a-clustering of bipolar LDI mass spectra (black) for 60 kW (75%) load of the research ship engine. The inorganic particle composition *via* LDI reveals distinct particle classes, *e.g.* soot particles indicated by carbon clusters C_n of both polarities. Of note, the PAH pattern from REMPI (red) is very similar for these particle groups, showing strong signals from alkylated phenanthrenes. Important PAH fragments appear at $m/z = 165$ and $m/z = 189$.

substances from laser desorption/ionization (LDI), similar to previous studies on light duty[54,55] and heavy-duty vehicles.[56] Fig. 1 shows the weight matrices (mass spectra of cluster centers) of the ART2a-clustering and regrouping of LDI mass spectra from 84 143 individual particles measured during engine operation with 60 kW (75%) load. The inorganic composition of the main particle types resembles previous experiments on truck engines,[56] with the majority of soot-dominated particles and peaks from organic fragments. Strong signals from Ca^+ and phosphate signatures can be attributed to lube oil residues.[56,57] Particle-bound Fe is resonantly ionized in our SPMS, leading to substantial signal enhancement.[41]

PAH signatures and their distribution over the particle ensemble

The new ionization method used here yields PAH mass spectra from about 50% of all ship emission particles in the current measurement. This equals the typical hit rate for PAHs with this technology[46] and thus suggests that the majority of detected particles contain PAHs. This is not surprising because a large fraction of the PAHs is in the gas phase after combustion and condenses on the particles when the temperature drops in the exhaust system. The average PAH mass spectra of the LDI-derived particle types are shown as red bars in Fig. 1. Independent of the particle type, the PAH mass spectra are dominated by a signal series in m/z sequences of 14 Da beginning at $m/z = 178$ – a profile that has previously been associated with ship engine emissions from distillate fuel operation, both in on-line measurements of the hot flue gas as well as in filter samples.[18,44,58] The peak at $m/z = 178$ can stem from both phenanthrene and anthracene; however, anthracene is nearly exclusively produced in the combustion process and has a lower degree of substitution.[60] The pronounced alkylation pattern in our experiments indicates the dominance of phenanthrene and its alkylated derivatives over anthracene. In piston engines, the combustion temperature determines the number of rings as well as the degree of substitution, *e.g.* alkylation,[59] and large diesel engines show higher alkylation degrees resulting from higher amounts of unburnt fuel.[23,44]

Of note, the average PAH signatures of all particle types are nearly identical, as apparent from the average PAH mass spectra in the respective groups (red bars in Fig. 1). In order to prove the stability of this signature among the individual particles – and therefore its suitability as a marker profile – we performed a statistical analysis of their homogeneity in the particle ensemble. The violin plots in Fig. 2 show the distribution of the congruence coefficients r_C for each 25 000 particle LDI mass spectra (blue) and the respective PAH mass spectra (red) according to

$$r_C = \frac{\sum_{i,j} x_{i,j} y_{i,j}}{\sqrt{\left(\sum_{i,j} x_{i,j}^2\right)\left(\sum_{i,j} y_{i,j}^2\right)}}$$

with x and y representing the individual mass spectra. The distribution of r_C as a measure of the similarity between mass

 © 2023 The Author(s). Published by the Royal Society of Chemistry

Open Access Article. Published on 12 July 2023. Downloaded on 11/22/2025 9:57:57 PM.
This article is licensed under a Creative Commons Attribution-NonCommercial 3.0 Unported Licence.

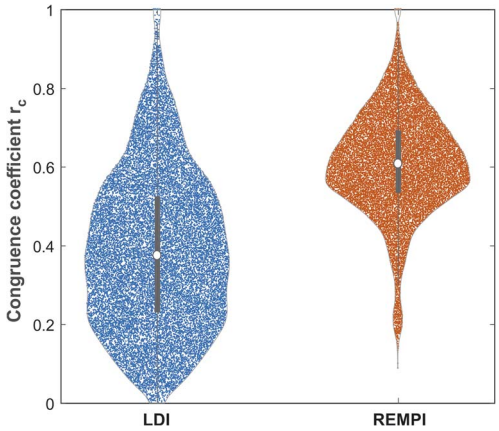

Fig. 2 Distribution of the congruence coefficients r_C between the single-particle mass spectra. The median r_C from the PAH mass spectra (white circle in the red probability density plot) is higher and its distribution is narrower compared to that from the LDI mass spectra of the same particles. The high similarity between PAH mass spectra supports their capability as a marker signature. Grey bars: interquartile range, $n = 25\,000$.

spectra shows that the individual PAH signatures are much more uniform than the signatures of the particle's inorganic composition from LDI. The higher similarity of PAH spectra is likely a result of incomplete combustion and imprints of the fuel signature, emphasizing the suitability of single-particle PAH spectra as fuel markers.

The effect of the particle size

SPMS yields the individual particle size; however, the optical detection efficiency drops rapidly for particles smaller than 200 nm, and thus, the instrument probes the fraction of the largest emitted particles. Of note, this size mode includes many particles of aged ship plumes in field applications[4] and coincides with the size of long-range transported particles.[61] Because of the instrument's bias towards large particles in conventional SPMS sizing mode, we performed additional experiments in the so-called free running mode that includes ultrafine particles. In this operation mode, the instrument's optical detection- and sizing unit is inactive and the desorption- and ionization lasers fire with a 100 Hz repetition rate into the particle beam, hitting particles on a random basis. Thus, the limits of optical particle detection can be overcome, however, at the cost of lost size information. Fig. 3(a) shows that the particle size distribution measured *via* a scanning mobility particle sizer (SMPS) peaks at around 80 nm. The SMPS-derived size distribution combined with the lower limit of SPMS spectrum generation at around 50 nm (ref. 62) suggests that particles between 50 and 150 nm size are dominant in the mass spectra measured in free running mode. Fig. 3(b) shows the average mass spectra of 5000 particles measured in free running mode in comparison to Fig. 3(c) where the average mass spectra of the same number of particles measured in conventional sizing mode are shown. The smaller particles measured in free running mode are soot-dominated and the larger particles show stronger phosphate and nitrate signals and more fragment peaks from organic carbon, *e.g.* in the PAH spectrum. This behavior can be attributed to a larger fraction of soot particles in the ultrafine mode and stronger contributions from lube oil and cold zones near the cylinder walls for the larger particles; see Toner *et al.*[56] The PAH mass spectra in free running mode show a slightly lower contribution from parent PAHs and fragments; the reason is not known. However, the PAH signature is still characterized by the intense homologue series of alkylated phenanthrenes. A cluster analysis of particle spectra in free running mode is provided in ESI, Fig. S1.†

The effect of the engine load

The third investigated key parameter with potential influence on the PAH signatures is the engine load, as shown by a direct

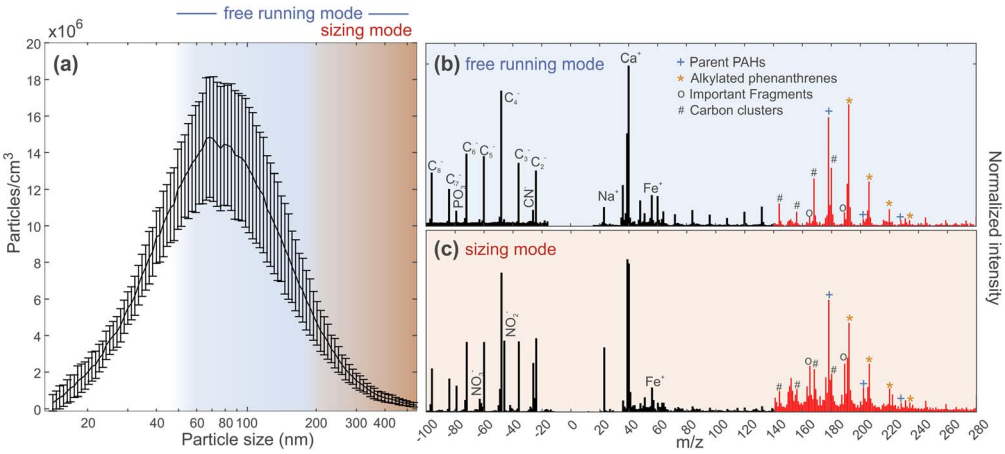

Fig. 3 (a) Particle size distribution of the research ship engine running on MGO at 60 kW load, measured by using a scanning mobility particle sizer (model 3082, TSI, U.S.). The blue shaded area illustrates the particle detection range of the SPMS in free running mode where particles of all sizes are hit at random, but size information from this instrument is not available. The red area indicates the coverage in normal sizing mode. The comparison of average mass spectra obtained in (b) free running mode (more smaller particles) and (c) in sizing mode (more larger particles) reveals that the characteristic series of alkylated phenanthrenes appears at all sizes. The additional series ($m/z = 231 + n \times 14$) is formed by fragments.[64]

Open Access Article. Published on 12 July 2023. Downloaded on 11/22/2025 9:57:57 PM.
This article is licensed under a Creative Commons Attribution-NonCommercial 3.0 Unported Licence.

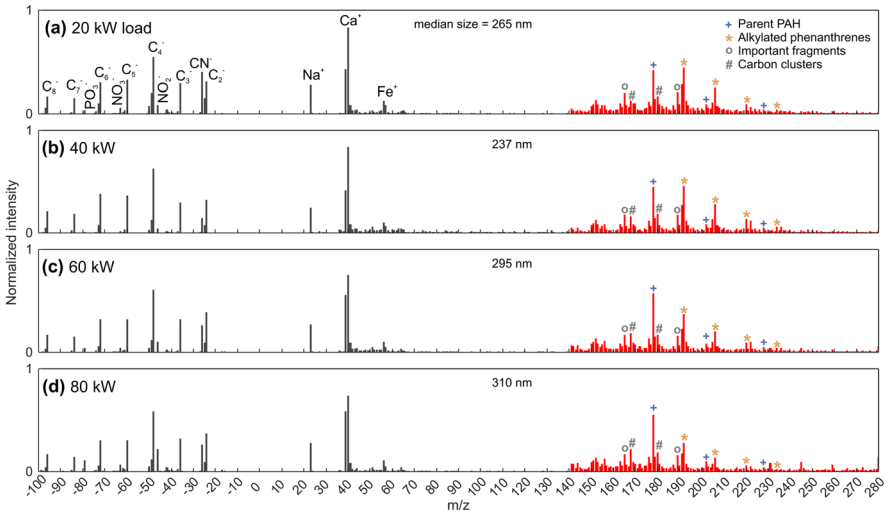

Fig. 4 With increasing engine load, the only noticeable change in the average PAH mass spectra (each $n = 3500$) is a subtle shift towards lighter PAHs. The pronounced alkylated phenanthrenes as the key feature indicating ship emissions from distillate fuels are hardly affected as well as the inorganic particle composition from LDI.

comparison of average mass spectra in Fig. 4. While the particle's organic content is highest at low load[18] and total PAH signals are slightly decreasing with increasing load (compensated by signal normalization as shown in Fig. 4), the general profile with strong alkylated phenanthrenes remains clearly visible. The inorganic composition reveals an increase in the nitrate signals with higher engine load and combustion temperature. The particle size distribution for all loads is given in ESI, Fig. S2.†

In summary, the vast majority of PAH-containing particles from MGO operation show a characteristic PAH pattern whose key feature, a dominant row from phenanthrene and its alkylated derivatives, is nearly unaffected by the particle type, size and engine load. The measured PAHs are a mixture of combustion products and residues of unburnt fuel and lube oil.[23,44] Spencer *et al.* found comparable PAH signatures in the majority of the droplets of sprayed diesel fuel using LDI-based SPMS.[63] Of note, the parent PAHs (*e.g.* $m/z = 178$) were nearly absent in this study as they originate from reactions between hydrocarbon radicals during combustion[59] while the alkylated species appear to be mainly fuel residues.[23] A further key difference between the droplet studies and our emission experiments is the much higher concentration of PAHs in the diesel fuel droplets,[10,18,63,64] and thus, they were detectable *via* LDI even in negative mode.[63]

We also investigated the diversity of PAH signatures by ART2a-clustering of single-particle REMPI mass spectra and analyzed the corresponding inorganic particle composition. Only a minority of particles produce substantially different PAH mass spectra, as shown in ESI, Fig. S3.†

Ship plume detection via PAHs in the field

To demonstrate the field applicability of our PAH-marker approach, we re-analyze subsets of the data from a field study at the Swedish coast in autumn 2019, see Passig *et al.*[50] for details. Briefly, we used the same SPMS system and the same configuration as in the laboratory but with additional particle concentration (see the "Methods" section above) to account for the general clean air conditions with less than 10 μg m^{-3} PM2.5. In the timeframe considered, circulating winds transported both terrestrial as well as marine aerosols to the sampling site (Fig. 5). From 292 242 chemically characterized particles in the period, 3746 particles showed PAH signals. Fig. S4 in the ESI† shows one of the resulting clusters exhibiting a PAH spectrum with dominant alkylated phenanthrenes, similar to the experimental results with the research ship engine. The corresponding inorganic composition from LDI reveals soot with Ca and Fe contributions, organic carbon (OC) peaks and some ageing signatures (*e.g.* $^{43}C_2H_3O^+$ contribution at $m/z = 43$). In order to investigate the sources of these particles, we correlated their appearance time with local wind data. Fig. 6(a) shows the distance from the intersection point of the wind trajectory with the main shipping lane to the measurement site as a function of time.

The wind speed is plotted in Fig. 6(b). The detection time and the size of all PAH-containing particles are depicted in Fig. 6(c) as grey dots, and the red dots represent the particles with dominant alkylated phenanthrenes. Obviously, these

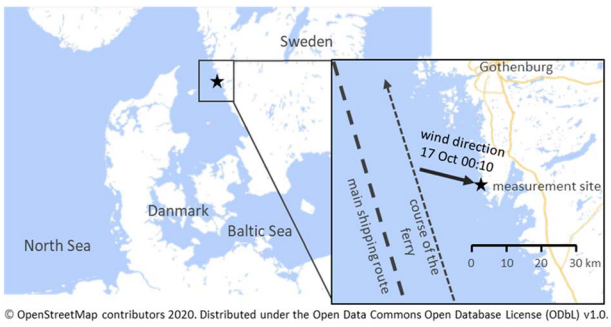

Fig. 5 Overview map of the region and the sampling site.

 © 2023 The Author(s). Published by the Royal Society of Chemistry

Open Access Article. Published on 12 July 2023. Downloaded on 11/22/2025 9:57:57 PM.
This article is licensed under a Creative Commons Attribution-NonCommercial 3.0 Unported Licence.

particles were mainly detected during periods of short distance travel to the ship lane and at low wind speeds, while at high wind speeds and especially during wind from land (distance > 100 km as shown in in Fig. 6(a)) they were only rarely detected. This behavior points to ship traffic as a probable source and indicates that land-based sources are of minor importance for this PAH signature.

Fig. 6(c) also shows a transient event of rather small particles (circled) indicating a single, less distant source. These particles also show the mentioned PAH profile but smaller peaks from OC, see ESI, Fig. S4(b)† for an average spectrum. Ship transponder data (AIS) revealed a ferry heading north at about 15–20 km distance to the sampling site 45 min before the event, see the inset of Fig. 5. The ferry traveled closer to the coastline than most other ships, and its lights were visible in the night. The ship was not equipped with a scrubber, so it is mandatory for it to use distillate fuel (*i.e.* MGO).

Complementarity with previous concepts

Our findings emphasize the potential of single-particle PAH measurements for ship plume detection and source apportionment of ship emissions. Previous SPMS approaches without PAH evaluation were based on a unique combination of transition metals from bunker fuel residues; however, the global change to cleaner fuels requires novel strategies.[65] Apart from transition metals, conventional SPMS can identify soot particles from many sources. However, it can hardly differentiate between the emissions from different engine types, although rather subtle changes in the SPMS mass spectra have been described.[54,56,63,66] The approach presented here focuses on organic fuel residues and combustion products, harnessing the high sensitivity for PAHs based on the resonant ionization process. Consequently, it reveals fuel and combustion characteristics beyond metals or lube oil additives. PAHs can also be detected with conventional SPMS, however, with less sensitivity and strong fragmentation that affects the reproducibility of mass spectra.[46,67–69]

Potential ambiguities and interferences with land-based diesel emissions

An important limitation could arise from interferences with other sources with potentially similar PAH emission profiles. Czech *et al.* performed gas phase analyses of PAHs from different sources emphasizing a unique profile of large (ship) diesel engines.[44] However, this study included the signatures of the lighter two-ring PAHs which are limited to the gas phase and not available here to differentiate between ship engines running on MGO and smaller diesel engines. Spencer *et al.* found comparable PAH signatures in lube oil and diesel droplets[63] where they have high concentrations,[64] but not in the exhaust emissions, probably because of lower sensitivity to PAHs in the LDI ionization used by their SPMS instrument.[68,70] A minor class of PAH-containing particles was determined in a study on heavy-duty vehicle emissions using the same instrument.[71] The

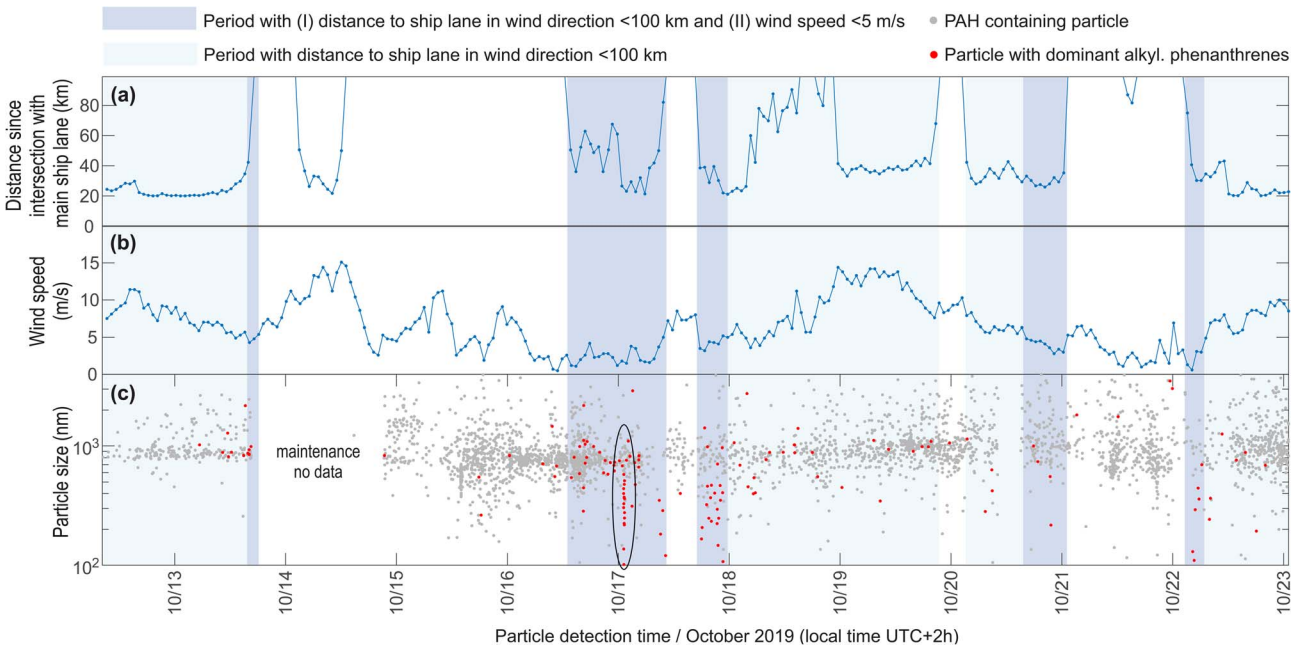

Fig. 6 Time course of wind data and particle detection events. (a) Distance from the measurement site to the main ship lane in the wind direction as derived from data of the local meteorological station. (b) Local wind speed from the same data. (c) Particle sizes and detection times for all PAH-containing particles (grey dots). The red dots represent PAH-containing particles with strong signals of alkylated phenanthrenes, belonging to the cluster shown in the ESI, Fig. S4(a).† Of note, the appearance of such particles is associated with light onshore winds and rather small distances to the ship lane in the wind direction (dark blue shaded periods). Only few particles of this type were detected in winds from the land, despite a motorway (20 km distance), the city of Gothenburg and active farming in the region. A transient signal of small particles from this type can even be attributed to an individual ship passage (circled).

Open Access Article. Published on 12 July 2023. Downloaded on 11/22/2025 9:57:57 PM. This article is licensed under a Creative Commons Attribution-NonCommercial 3.0 Unported Licence.

PAHs in these experiments were dominated by the four-ring parent PAHs at $m/z = 202$ in contrast to the strong alkylated phenanthrenes observed here for ship emissions.

We have conducted unpublished experiments with different kinds of logwood, biomass burning and brown coal so far; all of them have not produced similar PAH signatures, as shown in ESI, Fig. S5(a) and (b).† Using gas chromatography MS, Martens *et al.* found a ratio between phenanthrene and the sum of its alkylated derivatives of 2–6 for logwood and 0.4–4 for brown coal combustion,[72] while this factor is 0.4–1 in the experiments shown here, dependent on the engine load. However, in a preliminary experiment with a 5.7 kW diesel power generator, we observed PAH profiles comparable to that of the ship engine with MGO described here, see ESI, Fig. S5(c)† for a mass spectrum. We therefore assume that particles from diesel engines without exhaust cleaning devices bear the highest potential for interferences with the proposed ship emission markers. We expect that these interferences are of minor importance for two reasons: firstly, since most road traffic vehicles are nowadays equipped with particle filters, the quantity of land-based diesel particle emissions from such old cars, tractors, stationary engines, *etc.* is much lower compared to ship traffic emissions.[3] Secondly, if the measurements are performed close to the coastline during on-shore winds, *e.g.* for ship plume detection, particles of terrestrial origin reveal ageing markers in the SPMS. Actually, during our ambient air campaign with several thousand PAH-containing particles, the described pattern with dominant alkylated phenanthrenes was predominantly observed in soot particles during on-shore winds, as shown in Fig. 6.

Additional ambiguity arises from the different degradation dynamics of individual PAH compounds which have been discussed as a key limitation for the diagnostic ratio approach in source apportionment of PAHs.[73–75] However, the atmospheric residence time for the particles is in the range of minutes to a few hours before individual ship plumes disintegrate by dispersion and mixing.[76] We expect therefore, a limited effect of aging on the characteristic pattern of PAHs. Note that heterogeneous PAH degradation in the atmosphere is often much slower than in lab experiments,[77] for example, from shielding effects.[78,79]

Both the plume travel distance and wind speed are comparable to those of former experiments where resonant ionization of metals has been applied for sensitivity enhancement to Fe, Ni and V,[42,80] so it is a realistic scenario and detection range for optimized SPMS methods.

Conclusions

Our study showed the application of a new ionization method in SPMS to identify ship emission particles based on their PAH composition. The laboratory experiments indicate a high stability of the proposed marker signature throughout different particle types, engine loads and particle sizes. The respective particles can be found in ambient air and are associated with a marine background. Moreover, under appropriate wind conditions, individual plumes from ships running on MGO can be detected over a distance of several kilometers. A major ambiguity of this approach results from interferences with diesel-powered engines that not equipped with exhaust treatment. However, considering the local geography and weather conditions, these inaccuracies in source apportionment can easily be minimized.

To further emphasize the real-world application of the new PAH-based concept, future experiments will focus on many ship plumes in contrast to the occasional event presented here. Therefore, the optical particle detection of the instrument will be improved towards higher sensitivity and the measurement site will be closer to the shipping lane. This method is currently under evaluation for the identification of different types of distillate and residual fuels that gain importance with new regulations.[10,81] In combination with the resonant ionization of metals that substantially improves the detection of the traditional metal markers,[41,42] the approach could be generalized for the coverage and identification of all relevant ship fuels currently on the market. Further interesting applications will be the real-time measurement of ship plume ageing effects and PAH deposition in the surface water.

Author contributions

L. A., J. S., I. E. R., J. H. H and F. Y. Z. performed the SPMS experiments. L. A., J. S. and J. P. analyzed the data. T. K. B. and R. I. provided technical assistance. S. J., J. B., U. E., M. S. and M. R. S performed the aerosol characterization experiments at the engine. U. E. and B. B. provided the research ship engine and operated it. T. S., B. B. and R. Z. developed and managed the project and raised funding. J. S., C. W. H. C. and R. Z. participated in scientific discussions and provided expert advice. J. P. conceived the study, assisted with the experiments and wrote the manuscript.

Conflicts of interest

There are no conflicts to declare.

Acknowledgements

This research was supported by the German Federal Ministry for Economic Affairs and Climate Action (SAARUS project, grant no. 03SX483D), and by the Helmholtz Association (International Laboratory aeroHEALTH – Interlabs-0005). This research was funded by dtec.bw - Digitilization and Technology Research Center of the Bundeswehr (projects "LUKAS" and "MORE"). dtec.bw is funded by the European Union – NextGenerationEU. The authors want to thank Felix Lange (Langefreunde® Design Studio, Germany) for creating the Table of Contents Graphic.

References

1 EEA, *National emissions reported to the convention on long-range transboundary air pollution (LRTAP convention)*, https://www.eea.europa.eu/data-and-maps/data/national-emissions-reported-to-the-convention-on-long-range-

 © 2023 The Author(s). Published by the Royal Society of Chemistry

Open Access Article. Published on 12 July 2023. Downloaded on 11/22/2025 9:57:57 PM.
This article is licensed under a Creative Commons Attribution-NonCommercial 3.0 Unported Licence.

transboundary-air-pollution-lrtap-convention-13, accessed 22 August 2021.

2 International Transport Forum, *Reducing Sulphur Emissions from Ships: the Impact of International Regulation*, https://www.itf-oecd.org/reducing-sulphur-emissions-ships-impact-international-regulation-ships_5jlwvz8mqq9s-en, accessed 30 November 2020.

3 J. E. Jonson, M. Gauss, M. Schulz, J. P. Jalkanen and H. Fagerli, Effects of global ship emissions on European air pollution levels, *Atmos. Chem. Phys.*, 2020, **20**, 11399–11422.

4 S. Ausmeel, A. Eriksson, E. Ahlberg, M. K. Sporre, M. Spanne and A. Kristensson, Ship plumes in the Baltic Sea Sulfur Emission Control Area: chemical characterization and contribution to coastal aerosol concentrations, *Atmos. Chem. Phys.*, 2020, **20**, 9135–9151.

5 EPA, *Our Nation's Air*, https://gispub.epa.gov/air/trendsreport/2020/#home, accessed 22 August 2021.

6 N. Kuittinen, J. P. Jalkanen, J. Alanen, L. Ntziachristos, H. Hannuniemi, L. Johansson, P. Karjalainen, E. Saukko, M. Isotalo, P. Aakko-Saksa, K. Lehtoranta, J. Keskinen, P. Simonen, S. Saarikoski, E. Asmi, T. Laurila, R. Hillamo, F. Mylläri, H. Lihavainen, H. Timonen and T. Rönkkö, Shipping Remains a Globally Significant Source of Anthropogenic PN Emissions Even after 2020 Sulfur Regulation, *Environ. Sci. Technol.*, 2021, **55**, 129–138.

7 S. Jeong, J. Bendl, M. Saraji-Bozorgzad, U. Käfer, U. Etzien, J. Schade, M. Bauer, G. Jakobi, J. Orasche, K. Fisch, P. P. Cwierz, C. P. Rüger, H. Czech, E. Karg, G. Heyen, M. Krausnick, A. Geissler, C. Geipel, T. Streibel, J. Schnelle-Kreis, M. Sklorz, D. E. Schulz-Bull, B. Buchholz, T. Adam and R. Zimmermann, Aerosol emissions from a marine diesel engine running on different fuels and effects of exhaust gas cleaning measures, *Environ. Pollut.*, 2022, **316**, 120526.

8 IMO, *Annex VI of MARPOL 73/78, Regulations for the Prevention of Air Pollution from Ships Reg. 14*, https://www.imo.org/en/OurWork/Environment/Pages/Air-Pollution.aspx, accessed 30 August 2021.

9 A. Lähteenmäki-Uutela, J. Yliskylä-Peuralahti, S. Repka and J. Mellqvist, What explains SECA compliance: rational calculation or moral judgment?, *WMU Journal of Maritime Affairs*, 2019, **18**, 61–78.

10 A. Lunde Hermansson, I.-M. Hassellöv, J. Moldanová and E. Ytreberg, Comparing emissions of polyaromatic hydrocarbons and metals from marine fuels and scrubbers, *Transportation Research Part D: Transport and Environment*, 2021, **97**, 102912.

11 M. Sofiev, J. J. Winebrake, L. Johansson, E. W. Carr, M. Prank, J. Soares, J. Vira, R. Kouznetsov, J. P. Jalkanen and J. J. Corbett, Cleaner fuels for ships provide public health benefits with climate tradeoffs, *Nat. Commun.*, 2018, **9**, 406.

12 J. E. Jonson, M. Gauss, J. P. Jalkanen and L. Johansson, Effects of strengthening the Baltic Sea ECA regulations, *Atmos. Chem. Phys.*, 2019, **19**, 13469–13487.

13 C. Yu, D. Pasternak, J. Lee, M. Yang, T. Bell, K. Bower, H. Wu, D. Liu, C. Reed, S. Bauguitte, S. Cliff, J. Trembath, H. Coe and J. D. Allan, Characterizing the Particle Composition and Cloud Condensation Nuclei from Shipping Emission in Western Europe, *Environ. Sci. Technol.*, 2020, **54**, 15604–15612.

14 H. Winnes, E. Fridell and J. Moldanová, Effects of Marine Exhaust Gas Scrubbers on Gas and Particle Emissions, *J. Mar. Sci. Eng.*, 2020, **8**(4), 299.

15 P. Thor, M. E. Granberg, H. Winnes and K. Magnusson, Severe Toxic Effects on Pelagic Copepods from Maritime Exhaust Gas Scrubber Effluents, *Environ. Sci. Technol.*, 2021, **55**, 5826–5835.

16 D. R. Turner, I. M. Hassellöv, E. Ytreberg and A. Rutgersson, Shipping and the environment: Smokestack emissions, scrubbers and unregulated oceanic consequences, *Elementa - Sci. Anthrop.*, 2017, **5**(45), DOI: 10.1525/elementa.167.

17 J. Moldanová, E. Fridell, H. Winnes, S. Holmin-Fridell, J. Boman, A. Jedynska, V. Tishkova, B. Demirdjian, S. Joulie, H. Bladt, N. P. Ivleva and R. Niessner, Physical and chemical characterisation of PM emissions from two ships operating in European Emission Control Areas, *Atmos. Meas. Tech.*, 2013, **6**, 3577–3596.

18 T. Streibel, J. Schnelle-Kreis, H. Czech, H. Harndorf, G. Jakobi, J. Jokiniemi, E. Karg, J. Lintelmann, G. Matuschek, B. Michalke, L. Müller, J. Orasche, J. Passig, C. Radischat, R. Rabe, A. Reda, C. Rüger, T. Schwemer, O. Sippula, B. Stengel, M. Sklorz, T. Torvela, B. Weggler and R. Zimmermann, Aerosol emissions of a ship diesel engine operated with diesel fuel or heavy fuel oil, *Environ. Sci. Pollut. Res.*, 2017, **24**, 10976–10991.

19 Di Wu, Q. Li, X. Ding, J. Sun, D. Li, H. Fu, M. Teich, X. Ye and J. Chen, Primary Particulate Matter Emitted from Heavy Fuel and Diesel Oil Combustion in a Typical Container Ship: Characteristics and Toxicity, *Environ. Sci. Technol.*, 2018, **52**, 12943–12951.

20 J. J. Winebrake, J. J. Corbett, E. H. Green, A. Lauer and V. Eyring, Mitigating the Health Impacts of Pollution from Oceangoing Shipping: An Assessment of Low-Sulfur Fuel Mandates, *Environ. Sci. Technol.*, 2009, **43**, 4776–4782.

21 S. Oeder, T. Kanashova, O. Sippula, S. C. Sapcariu, T. Streibel, J. M. Arteaga-Salas, J. Passig, M. Dilger, H. R. Paur, C. Schlager, S. Mülhopt, S. Diabaté, C. Weiss, B. Stengel, R. Rabe, H. Harndorf, T. Torvela, J. K. Jokiniemi, M. R. Hirvonen, C. Schmidt-Weber, C. Traidl-Hoffmann, K. A. BéruBé, A. J. Wlodarczyk, Z. Prytherch, B. Michalke, T. Krebs, A. S. H. Prévôt, M. Kelbg, J. Tiggesbäumker, E. Karg, G. Jakobi, S. Scholtes, J. Schnelle-Kreis, J. Lintelmann, G. Matuschek, M. Sklorz, S. Klingbeil, J. Orasche, P. Richthammer, L. Müller, M. Elsasser, A. Reda, T. Gröger, B. Weggler, T. Schwemer, H. Czech, C. P. Rüger, G. Abbaszade, C. Radischat, K. Hiller, J. T. M. Buters, G. Dittmar and R. Zimmermann, Particulate matter from both heavy fuel oil and diesel fuel shipping emissions show strong biological effects on

Open Access Article. Published on 12 July 2023. Downloaded on 11/22/2025 9:57:57 PM.
This article is licensed under a Creative Commons Attribution-NonCommercial 3.0 Unported Licence.

human lung cells at realistic and comparable in vitro exposure conditions, *PLoS One*, 2015, **10**, e0126536.

22 F. Zhang, Y. Chen, C. Tian, D. Lou, J. Li, G. Zhang and V. Matthias, Emission factors for gaseous and particulate pollutants from offshore diesel engine vessels in China, *Atmos. Chem. Phys.*, 2016, **16**, 6319–6334.

23 O. Sippula, B. Stengel, M. Sklorz, T. Streibel, R. Rabe, J. Orasche, J. Lintelmann, B. Michalke, G. Abbaszade, C. Radischat, T. Gröger, J. Schnelle-Kreis, H. Harndorf and R. Zimmermann, Particle Emissions from a Marine Engine: Chemical Composition and Aromatic Emission Profiles under Various Operating Conditions, *Environ. Sci. Technol.*, 2014, **48**, 11721–11729.

24 M. Karl, J. E. Jonson, A. Uppstu, A. Aulinger, M. Prank, M. Sofiev, J. P. Jalkanen, L. Johansson, M. Quante and V. Matthias, Effects of ship emissions on air quality in the Baltic Sea region simulated with three different chemistry transport models, *Atmos. Chem. Phys.*, 2019, **19**, 7019–7053.

25 A. Seyler, F. Wittrock, L. Kattner, B. Mathieu-Üffing, E. Peters, A. Richter, S. Schmolke and J. P. Burrows, Monitoring shipping emissions in the German Bight using MAX-DOAS measurements, *Atmos. Chem. Phys.*, 2017, **17**, 10997–11023.

26 J. Mellqvist, J. Beecken, V. Conde and J. Ekholm, Surveillance of sulphur emissions from ships in Danish waters. *Report to the Danish Environmental Protection Agency*., **https://research.chalmers.se/publication/500251**, accessed 24 November 2020.

27 Y. Zhang, F. Deng, H. Man, M. Fu, Z. Lv, Q. Xiao, X. Jin, S. Liu, K. He and H. Liu, Compliance and port air quality features with respect to ship fuel switching regulation: a field observation campaign, SEISO-Bohai, *Atmos. Chem. Phys.*, 2019, **19**, 4899–4916.

28 S. Ausmeel, A. Eriksson, E. Ahlberg and A. Kristensson, Methods for identifying aged ship plumes and estimating contribution to aerosol exposure downwind of shipping lanes, *Atmos. Meas. Tech.*, 2019, **12**, 4479–4493.

29 S. Celik, F. Drewnick, F. Fachinger, J. Brooks, E. Darbyshire, H. Coe, J. D. Paris, P. G. Eger, J. Schuladen, I. Tadic, N. Friedrich, D. Dienhart, B. Hottmann, H. Fischer, J. N. Crowley, H. Harder and S. Borrmann, Influence of vessel characteristics and atmospheric processes on the gas and particle phase of ship emission plumes: in situ measurements in the Mediterranean Sea and around the Arabian Peninsula, *Atmos. Chem. Phys.*, 2020, **20**, 4713–4734.

30 F. Zhang, Y. Chen, C. Tian, X. Wang, G. Huang, Y. Fang and Z. Zong, Identification and quantification of shipping emissions in Bohai Rim, China, *Sci. Total Environ.*, 2014, **497–498**, 570–577.

31 V. Celo, E. Dabek-Zlotorzynska and M. McCurdy, Chemical Characterization of Exhaust Emissions from Selected Canadian Marine Vessels: The Case of Trace Metals and Lanthanoids, *Environ. Sci. Technol.*, 2015, **49**, 5220–5226.

32 X. Wang, Y. Shen, Y. Lin, J. Pan, Y. Zhang, P. K. K. Louie, M. Li and Q. Fu, Atmospheric pollution from ships and its impact on local air quality at a port site in Shanghai, *Atmos. Chem. Phys.*, 2019, **19**, 6315–6330.

33 K.-P. Hinz and B. Spengler, Instrumentation, data evaluation and quantification in on-line aerosol mass spectrometry, *J. Mass Spectrom.*, 2007, **42**, 843–860.

34 D. M. Murphy, The design of single particle laser mass spectrometers, *Mass Spectrom. Rev.*, 2007, **26**, 150–165.

35 K. A. Pratt and K. A. Prather, Mass spectrometry of atmospheric aerosols-recent developments and applications. Part II: on-line mass spectrometry techniques, *Mass Spectrom. Rev.*, 2012, **31**, 17–48.

36 J. Passig and R. Zimmermann, in *Photoionization and Photo-Induced Processes in Mass Spectrometry*, ed. R. Zimmermann and L. Hanley, Wiley-VCH, Weinheim, 2020.

37 R. M. Healy, I. P. O'Connor, S. Hellebust, A. Allanic, J. R. Sodeau and J. C. Wenger, Characterisation of single particles from in-port ship emissions, *Atmos. Environ.*, 2009, **43**, 6408–6414.

38 A. P. Ault, C. I. Gaston, Y. Wang, G. Dominguez, M. H. Thiemens and K. A. Prather, Characterization of the single particle mixing state of individual ship plume events measured at the Port of Los Angeles, *Environ. Sci. Technol.*, 2010, **44**, 1954–1961.

39 Z. Liu, X. Lu, J. Feng, Q. Fan, Y. Zhang and X. Yang, Influence of Ship Emissions on Urban Air Quality: A Comprehensive Study Using Highly Time-Resolved Online Measurements and Numerical Simulation in Shanghai, *Environ. Sci. Technol.*, 2017, **51**, 202–211.

40 Q. Xiao, M. Li, H. Liu, M. Fu, F. Deng, Z. Lv, H. Man, X. Jin, S. Liu and K. He, Characteristics of marine shipping emissions at berth: profiles for particulate matter and volatile organic compounds, *Atmos. Chem. Phys.*, 2018, **18**, 9527–9545.

41 J. Passig, J. Schade, E. I. Rosewig, R. Irsig, T. Kröger-Badge, H. Czech, M. Sklorz, T. Streibel, L. Li, X. Li, Z. Zhou, H. Fallgren, J. Moldanova and R. Zimmermann, Resonance-enhanced detection of metals in aerosols using single-particle mass spectrometry, *Atmos. Chem. Phys.*, 2020, **20**, 7139–7152.

42 J. Passig, J. Schade, R. Irsig, L. Li, X. Li, Z. Zhou, T. Adam and R. Zimmermann, Detection of Ship Plumes from Residual Fuel Operation in Emission Control Areas using Single-Particle Mass Spectrometry, *Atmos. Meas. Tech.*, 2021, **2021**, 4171–4185.

43 H. Czech, J. Schnelle-Kreis, T. Streibel and R. Zimmermann, New directions: Beyond sulphur, vanadium and nickel – about source apportionment of ship emissions in emission control areas, *Atmos. Environ.*, 2017, **163**, 190–191.

44 H. Czech, B. Stengel, T. Adam, M. Sklorz, T. Streibel and R. Zimmermann, A chemometric investigation of aromatic emission profiles from a marine engine in comparison with residential wood combustion and road traffic: implications for source apportionment inside and outside sulphur emission control areas, *Atmos. Environ.*, 2017, **167**, 212–222.

45 J. Passig, J. Schade, M. Oster, M. Fuchs, S. Ehlert, C. Jäger, M. Sklorz and R. Zimmermann, Aerosol Mass Spectrometer for Simultaneous Detection of Polyaromatic Hydrocarbons

 © 2023 The Author(s). Published by the Royal Society of Chemistry

Open Access Article. Published on 12 July 2023. Downloaded on 11/22/2025 9:57:57 PM.
This article is licensed under a Creative Commons Attribution-NonCommercial 3.0 Unported Licence.

and Inorganic Components from Individual Particles, *Anal. Chem.*, 2017, **89**, 6341–6345.

46 J. Schade, J. Passig, R. Irsig, S. Ehlert, M. Sklorz, T. Adam, C. Li, Y. Rudich and R. Zimmermann, Spatially Shaped Laser Pulses for the Simultaneous Detection of Polycyclic Aromatic Hydrocarbons as well as Positive and Negative Inorganic Ions in Single Particle Mass Spectrometry, *Anal. Chem.*, 2019, **91**, 10282–10288.

47 L. Mueller, G. Jakobi, H. Czech, B. Stengel, J. Orasche, J. M. Arteaga-Salas, E. Karg, M. Elsasser, O. Sippula, T. Streibel, J. G. Slowik, A. S. Prevot, J. Jokiniemi, R. Rabe, H. Harndorf, B. Michalke, J. Schnelle-Kreis and R. Zimmermann, Characteristics and temporal evolution of particulate emissions from a ship diesel engine, *Appl. Energy*, 2015, **155**, 204–217.

48 X. H. Song, P. K. Hopke, D. P. Fergenson and K. A. Prather, Classification of Single Particles Analyzed by ATOFMS Using an Artificial Neural Network, ART-2A, *Anal. Chem.*, 1999, **71**, 860–865.

49 C. M. Sultana, G. C. Cornwell, P. Rodriguez and K. A. Prather, FATES: a flexible analysis toolkit for the exploration of single-particle mass spectrometer data, *Atmos. Meas. Tech.*, 2017, **10**, 1323–1334.

50 J. Passig, J. Schade, R. Irsig, T. Kröger-Badge, H. Czech, T. Adam, H. Fallgren, J. Moldanova, M. Sklorz, T. Streibel and R. Zimmermann, Single-particle characterization of polycyclic aromatic hydrocarbons in background air in northern Europe, *Atmos. Chem. Phys.*, 2022, **22**, 1495–1514.

51 W. Zhao, P. K. Hopke and K. A. Prather, Comparison of two cluster analysis methods using single particle mass spectra, *Atmos. Environ.*, 2008, **42**, 881–892.

52 F. J. Romay, D. L. Roberts, V. A. Marple, B. Y. H. Liu and B. A. Olson, A High-Performance Aerosol Concentrator for Biological Agent Detection, *Aerosol Sci. Technol.*, 2002, **36**, 217–226.

53 SMHI, *Sveriges meteorologiska och hydrologiska institut*, **https://www.smhi.se/data/meteorologi/ladda-ner-meteorologiska-observationer#param=airtemperatureInstant**,stations=all,stationid=71190, accessed 2 September 2021.

54 D. A. Sodeman, S. M. Toner and K. A. Prather, Determination of Single Particle Mass Spectral Signatures from Light-Duty Vehicle Emissions, *Environ. Sci. Technol.*, 2005, **39**, 4569–4580.

55 J. Yang, S. Ma, B. Gao, X. Li, Y. Zhang, J. Cai, M. Li, L. Yao, B. Huang and M. Zheng, Single particle mass spectral signatures from vehicle exhaust particles and the source apportionment of on-line PM2.5 by single particle aerosol mass spectrometry, *Sci. Total Environ.*, 2017, **593–594**, 310–318.

56 S. M. Toner, D. A. Sodeman and K. A. Prather, Single Particle Characterization of Ultrafine and Accumulation Mode Particles from Heavy Duty Diesel Vehicles Using Aerosol Time-of-Flight Mass Spectrometry, *Environ. Sci. Technol.*, 2006, **40**, 3912–3921.

57 J. Lyyränen, J. Jokiniemi, E. I. Kauppinen and J. Joutsensaari, Aerosol characterisation in medium-speed diesel engines operating with heavy fuel oils, *J. Aerosol Sci.*, 1999, **30**, 771–784.

58 C. Radischat, O. Sippula, B. Stengel, S. Klingbeil, M. Sklorz, R. Rabe, T. Streibel, H. Harndorf and R. Zimmermann, Real-time analysis of organic compounds in ship engine aerosol emissions using resonance-enhanced multiphoton ionisation and proton transfer mass spectrometry, *Anal. Bioanal. Chem.*, 2015, **407**, 5939–5951.

59 M. Frenklach, Reaction mechanism of soot formation in flames, *Phys. Chem. Chem. Phys.*, 2002, **4**, 2028–2037.

60 J. T. Andersson and C. Achten, Time to Say Goodbye to the 16 EPA PAHs? Toward an Up-to-Date Use of PACs for Environmental Purposes, *Polycyclic Aromat. Compd.*, 2015, **35**, 330–354.

61 J. H. Seinfeld and S. N. Pandis, *Atmospheric Chemistry and Physics: from Air Pollution to Climate Change*, Wiley, 2016.

62 D. B. Kane and M. V. Johnston, Size and Composition Biases on the Detection of Individual Ultrafine Particles by Aerosol Mass Spectrometry, *Environ. Sci. Technol.*, 2000, **34**, 4887–4893.

63 M. T. Spencer, L. G. Shields, D. A. Sodeman, S. M. Toner and K. A. Prather, Comparison of oil and fuel particle chemical signatures with particle emissions from heavy and light duty vehicles, *Atmos. Environ.*, 2006, **40**, 5224–5235.

64 P. T. Williams, K. D. Bartle and G. E. Andrews, The relation between polycyclic aromatic compounds in diesel fuels and exhaust particulates, *Fuel*, 1986, **65**, 1150–1158.

65 G. Yu, Y. Zhang, F. Yang, B. He, C. Zhang, Z. Zou, X. Yang, N. Li and J. Chen, Dynamic Ni/V Ratio in the Ship-Emitted Particles Driven by Multiphase Fuel Oil Regulations in Coastal China, *Environ. Sci. Technol.*, 2021, **55**, 15031–15039.

66 S. M. Toner, L. G. Shields, D. A. Sodeman and K. A. Prather, Using mass spectral source signatures to apportion exhaust particles from gasoline and diesel powered vehicles in a freeway study using UF-ATOFMS, *Atmos. Environ.*, 2008, **42**, 568–581.

67 M. Bente, M. Sklorz, T. Streibel and R. Zimmermann, Online laser desorption-multiphoton postionization mass spectrometry of individual aerosol particles: molecular source indicators for particles emitted from different traffic-related and wood combustion sources, *Anal. Chem.*, 2008, **80**, 8991–9004.

68 R. Zimmermann, T. Ferge, M. Gälli and R. Karlsson, Application of single-particle laser desorption/ionization time-of-flight mass spectrometry for detection of polycyclic aromatic hydrocarbons from soot particles originating from an industrial combustion process, *Rapid Commun. Mass Spectrom.*, 2003, **17**, 851–859.

69 B. D. Morrical, D. P. Fergenson and K. A. Prather, Coupling two-step laser desorption/ionization with aerosol time-of-flight mass spectrometry for the analysis of individual organic particles, *J. Am. Soc. Mass Spectrom.*, 1998, **9**, 1068–1073.

70 F. Gunzer, S. Krüger and J. Grotemeyer, Photoionization and photofragmentation in mass spectrometry with visible and UV lasers, *Mass Spectrom. Rev.*, 2019, **38**, 202–217.

Open Access Article. Published on 12 July 2023. Downloaded on 11/22/2025 9:57:57 PM.
This article is licensed under a Creative Commons Attribution-NonCommercial 3.0 Unported Licence.

71 L. G. Shields, D. T. Suess and K. A. Prather, Determination of single particle mass spectral signatures from heavy-duty diesel vehicle emissions for PM2.5 source apportionment, *Atmos. Environ.*, 2007, **41**, 3841–3852.

72 P. Martens, H. Czech, J. Orasche, G. Abbaszade, M. Sklorz, B. Michalke, J. Tissari, T. Bizjak, M. Ihalainen, H. Suhonen, P. Yli-Pirilä, J. Jokiniemi, O. Sippula and R. Zimmermann, Brown Coal and Logwood Combustion in a Modern Heating Appliance: The Impact of Combustion Quality and Fuel on Organic Aerosol Composition, *Environ. Sci. Technol.*, 2023, **57**, 5532–5543.

73 K. Ravindra, R. Sokhi and R. van Grieken, Atmospheric polycyclic aromatic hydrocarbons: Source attribution, emission factors and regulation, *Atmos. Environ.*, 2008, **42**, 2895–2921.

74 M. Tobiszewski and J. Namieśnik, PAH diagnostic ratios for the identification of pollution emission sources, *Environ. Pollut.*, 2012, **162**, 110–119.

75 T. Miersch, H. Czech, A. Hartikainen, M. Ihalainen, J. Orasche, G. Abbaszade, J. Tissari, T. Streibel, J. Jokiniemi, O. Sippula and R. Zimmermann, Impact of photochemical ageing on Polycyclic Aromatic Hydrocarbons (PAH) and oxygenated PAH (Oxy-PAH/OH-PAH) in logwood stove emissions, *Sci. Total Environ.*, 2019, **686**, 382–392.

76 A. Petzold, J. Hasselbach, P. Lauer, R. Baumann, K. Franke, C. Gurk, H. Schlager and E. Weingartner, Experimental studies on particle emissions from cruising ship, their characteristic properties, transformation and atmospheric lifetime in the marine boundary layer, *Atmos. Chem. Phys.*, 2008, **8**, 2387–2403.

77 I. J. Keyte, R. M. Harrison and G. Lammel, Chemical reactivity and long-range transport potential of polycyclic aromatic hydrocarbons – a review, *Chem. Soc. Rev.*, 2013, **42**, 9333–9391.

78 M. Shrivastava, S. Lou, A. Zelenyuk, R. C. Easter, R. A. Corley, B. D. Thrall, P. J. Rasch, J. D. Fast, S. L. M. Simonich, H. Shen and S. Tao, Global long-range transport and lung cancer risk from polycyclic aromatic hydrocarbons shielded by coatings of organic aerosol, *Proc. Natl. Acad. Sci.*, 2017, **114**, 1246–1251.

79 P. A. Alpert, J. Dou, P. Corral Arroyo, F. Schneider, J. Xto, B. Luo, T. Peter, T. Huthwelker, C. N. Borca, K. D. Henzler, T. Schaefer, H. Herrmann, J. Raabe, B. Watts, U. K. Krieger and M. Ammann, Photolytic radical persistence due to anoxia in viscous aerosol particles, *Nat. Commun.*, 2021, **12**, 1769.

80 E. I. Rosewig, J. Schade, J. Passig, H. Osterholz, R. Irsig, D. Smok, N. Gawlitta, J. Schnelle-Kreis, J. Hovorka, D. Schulz-Bull, R. Zimmermann and T. Adam, Remote Detection of Different Marine Fuels in Exhaust Plumes by Onboard Measurements in the Baltic Sea Using Single-Particle Mass Spectrometry, *Atmosphere*, 2023, **14**(5), 849.

81 K. Lehtoranta, P. Aakko-Saksa, T. Murtonen, H. Vesala, L. Ntziachristos, T. Rönkkö, P. Karjalainen, N. Kuittinen and H. Timonen, Particulate Mass and Nonvolatile Particle Number Emissions from Marine Engines Using Low-Sulfur Fuels, Natural Gas, or Scrubbers, *Environ. Sci. Technol.*, 2019, **53**, 3315–3322.

 © 2023 The Author(s). Published by the Royal Society of Chemistry